Journal Pre-proof

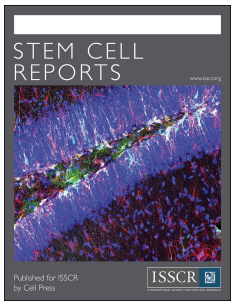

Human erythroid progenitors are directly infected by SARS-CoV-2: implications for emerging erythropoiesis in severe COVID19 patients.

Hector Huerga Encabo, William Grey, Manuel Garcia-Albornoz, Henry Wood, Rachel Ulferts, Iker Valle Aramburu, Austin G. Kulasekararaj, Ghulam Mufti, Venizelos Papayannopoulos, Rupert Beale, Dominique Bonnet

PII: S2213-6711(21)00052-7

DOI: https://doi.org/10.1016/j.stemcr.2021.02.001

Reference: STEMCR 1653

To appear in: *Stem Cell Reports*

Received Date: 22 January 2021

Revised Date: 29 January 2021

Accepted Date: 1 February 2021

Please cite this article as: Encabo, H.H., Grey, W., Garcia-Albornoz, M., Wood, H., Ulferts, R., Aramburu, I.V., Kulasekararaj, A.G., Mufti, G., Papayannopoulos, V., Beale, R., Bonnet, D., Human erythroid progenitors are directly infected by SARS-CoV-2: implications for emerging erythropoiesis in severe COVID19 patients. *Stem Cell Reports* (2021), doi: https://doi.org/10.1016/j.stemcr.2021.02.001.

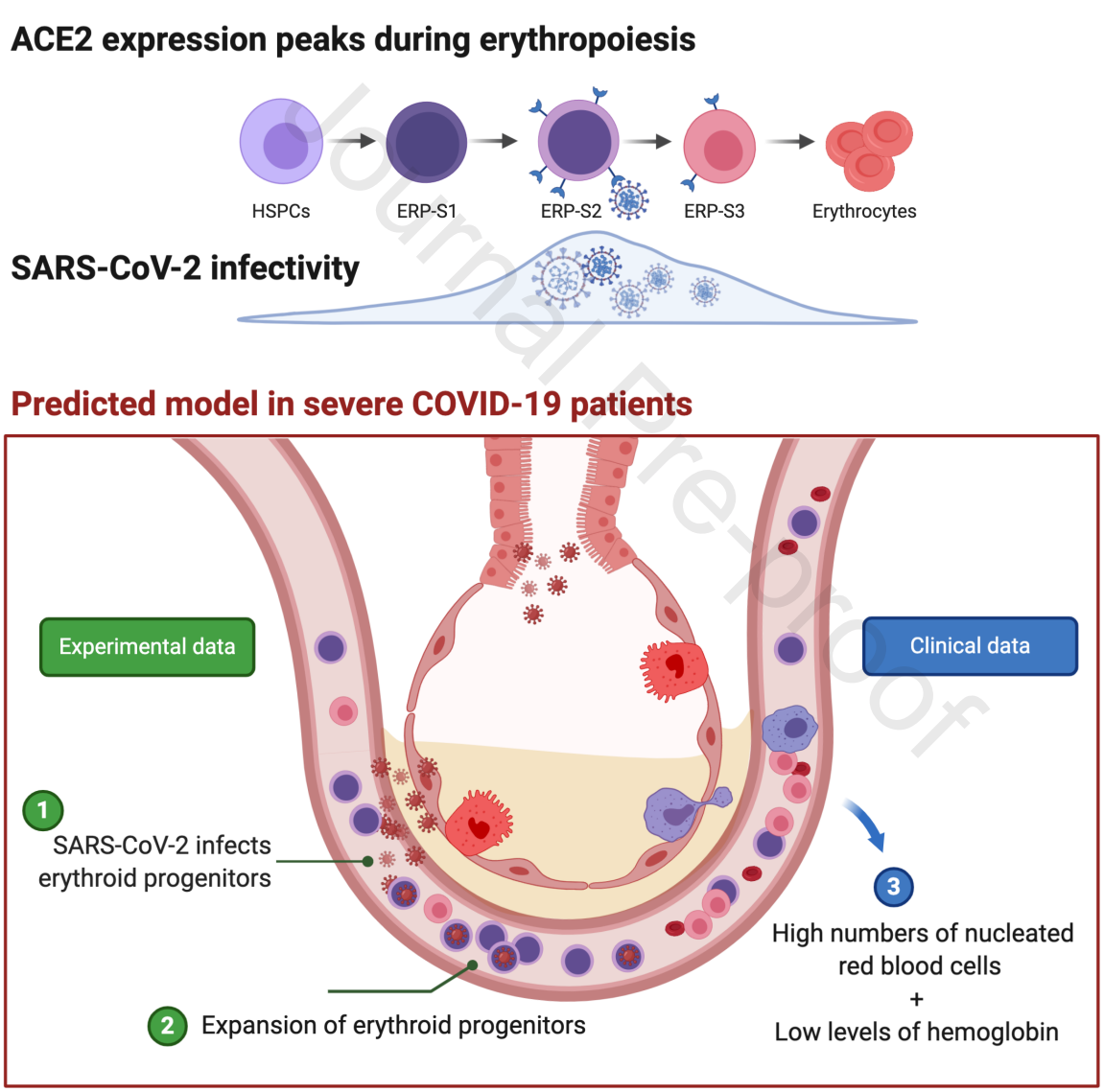

Human erythroid progenitors are directly infected by SARS-CoV-2: implications for emerging erythropoiesis in severe COVID19 patients.

Hector Huerga Encabo[1], William Grey[1*], Manuel Garcia-Albornoz[1*], Henry Wood[1,2], Rachel Ulferts[3], Iker Valle Aramburu[4], Austin G. Kulasekararaj[2], Ghulam Mufti[2], Venizelos Papayannopoulos[4], Rupert Beale[3] and Dominique Bonnet[1].

1- Haematopoietic Stem Cell Laboratory, The Francis Crick Institute, London, NW1 1AT, UK
2- Department of Haematology, King's College Hospital, London, SE5 9RS, UK
3-Cell Biology of infection laboratory, The Francis Crick Institute, London NW1 1AT, UK
4- Antimicrobial defense laboratory, The Francis Crick Institute, London NW1 1AT, UK

*: These authors have contributed equally.

Corresponding author: Prof Dominique Bonnet, Haematopoietic Stem Cell Laboratory, The Francis Crick Institute, 1 Midland Road, London, NW1 1AT, UK

Email address: Dominique.bonnet@crick.ac.uk

Keywords: SARS-CoV.2; human Hematopoietic stem/progenitor cells; erythropoiesis; anemia, hypoxia

SUMMARY

We document here that intensive care COVID19 patients suffer a profound decline in hemoglobin levels but show an increase of circulating nucleated red cells, suggesting that SARS-CoV-2 infection either directly or indirectly induces stress erythropoiesis. We show that ACE2 expression peaks during erythropoiesis and renders erythroid progenitors vulnerable to infection by SARS-CoV-2. Early erythroid progenitors, defined as $CD34^{-}$ $CD117^{+}CD71^{+}CD235a^{-}$, show the highest levels of ACE2 and constitute the primary target cell to be infected during erythropoiesis. SARS-CoV-2 causes the expansion of colony formation by erythroid progenitors and can be detected in these cells after two weeks of the initial infection. Our findings constitute the first report of SARS-CoV-2 infectivity in erythroid progenitor cells and can contribute to understanding both the clinical symptoms of

severe COVID19 patients and how the virus can spread through the circulation to produce local inflammation in tissues, including the bone marrow.

INTRODUCTION

The severe acute respiratory syndrome coronavirus 2 (SARS-CoV-2) has infected and spread globally amongst humans, causing a pandemic crisis. The resulting Corona Virus Disease 2019 (COVID-19) is a spectrum of responses to SARS-CoV-2 infection, from asymptomatic individuals to severe disease and mortality (Guan et al., 2020).

The mechanism of infection by SARS-CoV-2 is fairly well characterized. For viral entry, the binding between the viral surface spike glycoprotein (S) and target cell surface angiotensin-converting enzyme-2 (ACE2) followed by cleavage of S by the transmembrane protease serine 2 (TMPRSS2) are required (Walls et al., 2020). ACE2 expression has been extensively reported in different epithelial cells from the respiratory tract, constituting the main infection site of SARS-CoV-2 (Lukassen et al., 2020).

Further reports demonstrate ACE2 expression in cells from other tissues such as intestinal epithelial cells, hepatocytes and neurons, making these cells vulnerable to be infected by SARS-CoV2 (Pellegrini et al., 2020; Sungnak et al., 2020; Wang et al., 2020; Zhang et al., 2020). In line with these findings, increasing evidence of gastrointestinal, hepatic and neurological symptoms have been reported (Varatharaj et al., 2020; Wu et al., 2020; Yang and Tu, 2020). More recently, an aberrant increase of erythroid progenitors in circulation have been reported, especially in severe cases (Bernardes et al., 2020). Indeed, this observation together with hypoxia, anemia and coagulopathies highly correlate with severity and mortality (Bernardes et al., 2020; Vabret et al., 2020). Disruption of erythropoiesis may be an indirect effect of the systemic hyperinflammation that occurs in intensive care patients. Another potential explanation is that direct targeting of hematopoietic stem/progenitor cells

(HSPCs) and/or erythroid progenitors (ERP) by SARS-CoV-2 contributes to the hematological features of COVID-19. It has previously been suggested that SARS-CoV-2 can have a tropism for blood cells (Cavezzi et al., 2020). More recently, HSCs from cord blood have been reported to express ACE2 and exposure to the Spike protein can reduce their functionality (Ropa et al., 2020). Despite these observations, the infectivity of SARS-CoV-2 in HSPCs and more particularly in erythroid progenitors have not been characterized. In this report, we have studied HSPCs and different erythroid progenitor populations to assess if they can be infected by SARS-CoV-2.

RESULTS

Patients treated for severe COVID-19 (as defined by requirement for intensive care admission) at King's College Hospital (London, UK) show a rapid and profound decline in hemoglobin following admission (**Figure 1A**). Interestingly, this is associated with the appearance of circulating nucleated red cells, peaking between 2-3 weeks after admission (**Figure 1B**). Numbers of white cells and platelets rise over this period, indicating that the anemia is not associated with myelosuppression (**Figure S1A-B**).

Publicly available datasets indicate that ACE2 and TMPRSS2 expression is scarce among hematopoietic cell types, and absent on human HSPCs. Of note, progenitors of the erythroid lineage appear to be the only cell types expressing both ACE2 and TMPRSS2 among the cells present in the bone marrow (The Human Cell Atlas Bone Marrow Single-Cell Interactive Web Portal). Intrigued by this observation, we used detailed datasets of in vitro human erythropoiesis (Gillespie et al., 2020) to characterize ACE2 expression from hematopoietic stem and progenitor cells (HSPCs), $CD34^{+}$ cells, to mature erythrocytes. We found that ACE2 expression peaks during erythropoiesis (**Figure 1C**). During the first days of erythropoiesis ACE2 is not expressed, starting to be expressed around day 6-7, before

reaching its maximum level of expression at day 10-11 and then declining until the last time point at day 16. Therefore, we can distinguish 3 stages of ACE2 expression, where Stage 1 (S1) represents the initial time points with no ACE2 expression, Stage 2 (S2) represents the time points where ACE2 expression increases and reaches maximum levels and Stage 3 (S3) represents the last time points where ACE2 expression is declining and at low levels. Accordingly, in our analysis of the differentially expressed genes among these three stages, ACE2 appeared as one of the top upregulated genes in Stage 2 (**Figure S1C**). Interestingly, these three stages coincide with three clusters observed by the dimensionality reduction analysis during the erythroid differentiation (**Figure 1D**). S1 differentially expressed genes include stem and early progenitor markers such as CD34, CD38 and RUNX1. In S2, these markers disappear and erythroid-committed progenitor markers like CD71 and MYB are upregulated. Finally, in S3, GATA1 and KLF1 target genes are enriched (**Figure S1C-D, Supplementary Table 1**) as expected in late and terminal erythroid differentiation (Ludwig et al., 2014).

Based on the expression of different surface markers frequently used in flow cytometry to isolate different erythroid progenitors (Chen et al., 2009; Mello et al., 2019; Westers et al., 2017), we defined three erythroid progenitor populations (ERP) in order to isolate S1-S3 from different tissues (**Figure 1E**). Erythroid progenitors of Stage 1 (ERP-S1) can be defined as $CD34^{+}CD117^{+}CD71^{+}CD235a^{-}$, ERP-S2 as $CD34^{-}CD117^{+}CD71^{+}CD235a^{-}$ and ERP-S3 as $CD34^{-}CD117^{-}CD71^{+}CD235a^{+}$ (**Figure 1F**). Of note, using another independent dataset we also observed that ACE2 expression is higher in erythroid progenitors when defined as $CD71^{+}CD235a^{-}$, further validating our strategy to enrich for $ACE2^{+}$ erythroid progenitors (Ludwig et al., 2019).

We characterized and measured the abundance of ERP-S1, ERP-S2 and ERP-S3 in cord blood, bone marrow and peripheral blood (**Figure 1G**). As expected, all types of erythroid

progenitors are more abundant in the bone marrow. Nonetheless, due to the possible impact as a SARS-CoV-2 chaperone, is worth highlighting that $ACE2^{+}$ erythroid progenitors are also present in peripheral blood (**Figure S1E**).

From bone marrow aspirates of human healthy donors, we used our markers to isolate the 3 ERP populations by cell sorting, determine the expression of ACE2 and TMPRSS2 and evaluate their susceptibility to infection by SARS-CoV-2 (**Figure 2A**). As expected, when we analyzed the expression of ACE2 at the RNA level, the ERP-S2 population showed the highest level of expression while ERP-S3 showed low levels and both ERP-S1 and HSPCs showed no expression of ACE2 (**Figure S2A**). More importantly at the protein level, the immunofluorescence analysis of the different ERP populations confirmed that ACE2 and TMPRSS2 are co-expressed in the ERP-S2 cells (**Figure 2B, Figure S2B-C**). Notably, we also detected a subset of ERP-S3 cells that co-expressed ACE2 and TMPRSS2, while we did not detect any cell in the ERP-S1 and HSPCs populations showing ACE2/TMPRSS2 co-expression (**Figure 2B, Figure S2B-C**).

We then performed infection assays on bone marrow HSPCs and the three ERP populations. To analyze the capacity of the virus to directly infect these cells, we measured different viral genes by real time quantitative PCR (RT-qPCR) in the different populations after being in the presence of SARS-CoV-2. Interestingly, we observed that ERP-S2 cells are highly susceptible to SARS-CoV-2 infection, as shown by the detection of different viral genes after 24 hours of infection (**Figure 3A**). In contrast, HSPCs and ERP-S1 cells are completely refractory to infection by SARS-CoV-2, as we cannot detect any trace of the virus in these cells. In keeping with the ACE2/TMPRSS2 cell surface levels, we also detected viral genome in ERP-S3 cells, although at a lower level, indicating that erythroid progenitors in this stage of differentiation are also susceptible to infection. To address the question of whether SARS-CoV-2 is not only able to bind to ERP-S2 cells (and to a lesser extent to ERP-S3 cells), but is

also capable of replicating inside these progenitor cells, we analyzed the difference in the viral genome load between 30 minutes (where we just detect viruses putatively attached to cells) and 24 hours (where we also quantify viruses amplified inside cells) after exposure. Importantly, our results showed that SARS-CoV-2 can infect and amplify its genome in erythroid progenitors of Stage 2 and Stage 3 but is not able to bind and infect HSPCs from the bone marrow (**Figure 3B**). To reproduce more physiological scenarios, we also infected the erythroid progenitors from peripheral blood from healthy individuals at lower MOI and we obtained similar results (**Figure S3A**). We next performed colony-forming unit (CFU) assay to analyze how the exposure to SARS-CoV-2 could influence the functionality of these erythroid progenitor populations. As expected, ERP-S1 and ERP-S2 are able to generate colonies, unlike the more differentiated ERP-S3 population, and ERP-S1 are more prompted to generate BFU-E colonies while ERP-S2 are more prompted to generate CFU-E colonies (**Figure S3B)**. After being in the presence of SARS-CoV-2, both erythroid progenitor populations produce more colonies (**Figure 3C)**. We were intrigued by the possibility that after the two weeks of CFU experiment the virus could remain in these cells/colonies. To address this question, we picked independent colonies from ERP-S1 or ERP-S2 plates and analyzed the presence of SARS-Cov-2 virus by RT-qPCR. While we were not able to amplify viral genes in any colony from ERP-S1 (0 out of 10 in two independent experiment), we detected the virus in ~90% of the colonies from ERP-S2 (**Figure 3D, Figure S3C**) [9 out of 10 in experiment 1 and 8/10 in experiment 2 (data not shown)]. Interestingly, these results indicate that SARS-CoV-2 remains in ERP-S2 after 14 days of the initial infection.

DISCUSSION

The COVID-19 pandemic continues to constitute a huge threat to public health worldwide. Despite the efforts and advances to untangle the mechanisms of SARS-CoV-2 infection and

transmission among humans, we are still blind to the overall COVID-19 pathology and its consequences. The results we present here might help understand the emergent erythropoiesis and aberrant presence of erythroid progenitors in the peripheral blood of severe COVID-19 patients (Bernardes et al., 2020; Shahbaz et al., 2020). These recent evidences indicate that the increase of erythroid progenitors in circulation constitute a hallmark of both severity and fatality in COVID-19 patients (Bernardes et al., 2020; Shahbaz et al., 2020). In this context, our observations that the virus can be detected after 14 days in the ERP-S2 without impairing their viability, rather causing an increase of colonies, suggest that the expansion of circulating erythroid cells that have been reported in severe patients may be due to direct infection of upstream $CD71^{+}CD235a^{-}$ progenitors. In depth research will be key to elucidate which of these two events, direct infection of erythroid progenitors and pathological increase of these populations in the bloodstream, occur first in vivo in patients. Our results also open the question about the causality between direct SARS-CoV-2 infection of erythroid progenitors and clinical manifestations resulting from hemoglobin decline and anemia. In light of our findings, we cannot discard the possibility that these symptoms are not simply a byproduct of inflammation and overall poor health and that, instead, direct infection of erythroid progenitors by SARS-CoV-2 contributes to this aberrant erythropoiesis.

The results we show here constitute the first evidence of direct infection of specific erythroid progenitors, named as ERP-S2 ($CD71^{+}CD235A^{-}$) and ERP-S3 ($CD71^{+}CD235a^{+}$), by SARS-CoV-2. Especially relevant is the high ability (or facility) of the virus to infect ERP-S2, the most vulnerable erythroid progenitor population. Based on previous works and our observations, ERP-S2 population includes colony forming units-erythroid (CFU-E) cells and early pro-erythroblast cells (Ludwig et al., 2019; Westers et al., 2017). Considering their high proliferative capacity, the infection of these progenitors by SARS-CoV-2 may have a major detrimental impact not only in erythropoiesis, but also in the spread of the virus through

millions of circulating infected cells. Also, this presents a scenario in which infected erythroid progenitors may cause local inflammation in the bone marrow, which could cause a drastic disruption of hematopoiesis and the production of immune cells.

In contrast to the observations in erythroid progenitors, we report that bone marrow HSPCs ($CD34^{+}CD38^{-}$) do not express ACE2 and TMPRSS2 at the RNA or protein level. Consequently, we show that HSPCs are not infected by SARS-CoV-2.

In this report, we also provide clinical data of a cohort of 30 COVID-19 patients that were treated in intensive care units (ICU) at King's College London. We show that the decline in hemoglobin levels coincides with an aberrant increase of nucleated red blood cells in circulation. These nucleated red blood cells correspond to ERP-S3 cells (Shahbaz et al., 2020). Similar to what we show here, Shahbaz and colleagues also report that this population can be infected by SARS-CoV-2 and that the infection induces the immunosuppressive capacity of these cells. Of note, they did not analyze the population that we characterize here as ERP-S2, the more upstream progenitor population, which is more susceptible to infection ($CD71^{+}CD235a^{-}$). Importantly, our results might also have an impact in our understanding of the transmission and incubation period of SARS-CoV-2, as different levels of infected progenitors in the bloodstream could greatly alter such parameters. Finally, identification of infected ERP-S2 populations in hospitalized patients could help identify those patients that will suffer from severe hematopathology, potentially allowing pre-emptive management strategies to improve outcomes.

EXPERIMENTAL PROCEDURES

Clinical data

A sample of 30 patients who were being treated for COVID-19 on intensive care units at King's College Hospital on 1st May 2020, and who had first tested positive for SARS-CoV-2

by polymerase chain reaction within 7 days of admission to hospital, was identified using information from the hospital's Business Intelligence Unit and electronic patient record (EPR) system. Values for peripheral blood hemoglobin concentration, white blood cell count, platelet count and nucleated red blood cell percentage on the day of presentation to hospital and subsequent 28 days were collected from the EPR system. In cases where multiple tests were performed in the same day, the first value was collected.

RNAseq data import and analysis of ACE2 expression

RNAseq dataset was downloaded from GEO database (GEO accession number GSE118537). Differential gene expression analysis between erythroid subpopulations was performed using DEseq2 methodology on a pair-wise comparison fashion. All genes with and adjusted p value < 0.05 were considered as statistically significant between two subpopulations. Each of the three ERP population was compared with the other two and those genes differentially expressed in both comparisons were considered as differentially expressed for the specific subpopulation. Top 300 upregulated genes in each ERP population are listed in Supplementary Table 1.

Isolation of mononuclear cells from human cord blood, bone marrow and peripheral blood

Umbilical Cord Blood (UCB) was obtained from full term donors after informed consent at the Royal London Hospital (London, U.K.). Mononuclear cells (MNCs) were isolated by density centrifugation using Ficoll-Paque (GE 67 Healthcare). Human bone marrow mononuclear cells were obtained from StemCell Technologies (Cat#70001). Peripheral blood was isolated from consenting unscreened healthy adult volunteers following approved protocols by the ethics board of the Francis Crick Institute and the regulations of the Human

Tissue act 2004. Peripheral blood mononuclear cells (PBMCs) were isolated by centrifugation over a Histopaque-1119 gradient (Sigma-Aldrich 11191).

mRNA quantification by RT-qPCR

Total RNA was extracted using the RNeasy Microkit (Qiagen, Cat# 74004), and the RNA was retrotranscribed using the SuperScript III First-Strand Synthesis system (Thermo Fisher Scientific, Cat# 18080051). For RT-qPCR, PowerUP SYBR Green (Applied Biosystems, Cat# 15310939), MicroAmp Optical 384-Well Reaction Plate (Applied biosystems, Cat# 4309849), and the Applied Biosystems QuantStudio 7 were used according to the instructions provided by the manufacturers. For the detection of SARS-CoV-2 we used previously validated primers (Corman et al., 2020). See primers used in Supplementary Information.

Flow cytometry analysis and cell sorting

All experiments were analyzed at the Flow Cytometry core facility of The Francis Crick Institute using the LSR FORTESSA (BD Biosciences) equipped with a 488-nm laser, a 561-nm laser, a 633-nm laser, and a 405-nm laser. For sorting, cell suspensions were filtered through a 35-µm nylon mesh (Falcon, Cat# 352235) and sorted in a BD FACS FUSION cell sorter equipped with 488-nm, 561-nm, 633-nm, and 405-nm lasers. See antibodies used in Supplementary Information. All experiments were analyzed with FACSDiva 6.2 (BD Biosciences) and FCS Express 7 software.

Immunostaining, confocal microscopy and immunofluorescence quantification

Polyclonal goat anti-ACE2 antibody (R&D Systems, Cat#AF933) at 15 µg/ml and polyclonal rabbit anti-TMPRSS2 (ThermoFisher, Cat#PA5-14264) at 15 µg/ml were used for the primary antibody incubation. Donkey anti-goat Alexa 647 (Invitrogen, Cat#A21447) and

donkey anti-rabbit Alexa488 (Invitrogen, Cat#A21206) were used at 10 µg/ml for the secondary antibody staining. Fluorescence imaging was performed at a Leica TCS SP5 inverted confocal microscope using the sequential scan in between frames mode with a 63x objective. Background signal was accounted for by performing secondary only staining controls. Fiji/ImageJ version 2.0.0 software was used for image analysis. Fluorescence intensity quantifications were done by selecting individual cells using an intensity-based mask at the DAPI channel of at least five different representative regions of interest per group of cells. This mask was then applied for the quantification of fluorescence intensity in the 488 channel (TMPRSS2) and the 647 channel (ACE2).

SARS-CoV-2 production and infection

Vero E6 cells (a kind gift from Oliver Schwarz, Institute Pasteur, Paris) were maintained in DMEM modified with high glucose, L-glutamine, phenol red and sodium pyruvate (ThermoFisher, Cat#41966-029) supplemented with 10% FCS. SARS-CoV-2 strain BetaCoV/England/02/2020 (obtained from Public Health England) was propagated at 37°C on VeroE6 cells in DMEM supplemented with 2% FCS. The titer was determined by plaque assay as follows: confluent monolayers of VeroE6 cells grown on 6-well plates were incubated with 200 µl of a 10-fold serial dilution of virus stock in DMEM supplemented with 10% FCS for 1 h at room temperature. The cells were then overlaid with 0.5x DMEM supplemented with 1% FCS and 1.2% Avicel (BMC Biopolymers, Belgium). After 4d incubation at 37℃, cells were fixed with 4% formaldehyde in PBS followed by staining with 0.1% toluidine blue (Sigma, Cat#89640). The titer was calculated as plaque forming units (PFU) per ml. Hematopoietic cells were infected with SARS-CoV-2 at a multiplicity of infection (MOI) of 5 PFU per cell. Cells were washed three times with PBS to remove unbound virus prior to lysis for RNA isolation.

Colony-forming Unit (CFU) assay

After 24 hours of infection cells were seeded for 2 weeks in methylcellulose-based medium with recombinant cytokines for human cells (StemCell Technologies, Cat#04435). Two independent experiments with 2-3 biological donors in each experiment were analyzed to assess the number of colony-forming unit in each cell population.

Statistical analysis

Statistical methods relevant to each figure are outlined in the figure legend. Sample size was not predetermined. Data are presented as means with standard deviation (SD) to indicate the variation within each experiment. A two-way ANOVA test was used for the comparison between the different cell populations.

Acknowledgments

We want to thank staffs at the Flow Cytometry core facility of the Francis Crick Institute for their valuable help. We also want to thank Drs Syed Mian, Sonia Tejedor and Giuliana Magri for their constructive discussion on the paper. This work was supported by the Francis Crick Institute, which receives its core funding from Cancer Research UK (FC001045), the UK Medical Research Council (FC001045) and the Wellcome Trust (FC001045) to DB. For the purpose of Open Access, the author has applied a CC BY public copyright licence to any Author Accepted Manuscript version arising from this submission.

AUTHOR CONTRIBUTIONS

Conceptualization: HHE, WG and DB; Methodology: HHE, WG, RU, and IVA; Analysis

and interpretation: HHE, WG, MGA, HW, RU, IVA, and DB; Patients data analysis: AGK, GM and HW; Writing paper: HHE and DB; Review & Editing paper: HHE, WG, MGA, HW, VP, RB and DB; Funding Acquisition: DB.

DECLARATION OF INTERESTS

The authors declare no competing interests.

REFERENCES

Bernardes, J.P., Mishra, N., Tran, F., Bahmer, T., Best, L., Blase, J.I., Bordoni, D., Franzenburg, J., Geisen, U., Josephs-Spaulding, J., et al. (2020). Longitudinal multi-omics analyses identify responses of megakaryocytes, erythroid cells and plasmablasts as hallmarks of severe COVID-19 trajectories. Immunity. 53(6), 1296-1314.e9.

Cavezzi, A., Troiani, E., and Corrao, S. (2020). COVID-19: hemoglobin, iron, and hypoxia beyond inflammation. A narrative review. Clin. Pract. *10(2)*.

Chen, K., Liu, J., Heck, S., Chasis, J.A., An, X., and Mohandas, N. (2009). Resolving the distinct stages in erythroid differentiation based on dynamic changes in membrane protein expression during erythropoiesis. Proc. Natl. Acad. Sci. U. S. A. *106*, 17413–17418.

Corman, V.M., Landt, O., Kaiser, M., Molenkamp, R., Meijer, A., Chu, D.K., Bleicker, T., Brünink, S., Schneider, J., Luisa Schmidt, M., et al. (2020). Detection of 2019 -nCoV by RT-PCR. Euro Surveill *25*, 1–8.

Gillespie, M.A., Palii, C.G., Sanchez-Taltavull, D., Shannon, P., Longabaugh, W.J.R., Downes, D.J., Sivaraman, K., Espinoza, H.M., Hughes, J.R., Price, N.D., et al. (2020). Absolute Quantification of Transcription Factors Reveals Principles of Gene Regulation in Erythropoiesis. Mol. Cell *78*, 960-974.e11.

Guan, W., Ni, Z., Hu, Y., Liang, W., Ou, C., He, J., Liu, L., Shan, H., Lei, C., Hui, D.S.C., et al. (2020). Clinical Characteristics of Coronavirus Disease 2019 in China. N. Engl. J. Med. *382*, 1708–1720.

Ludwig, L.S., Gazda, H.T., Eng, J.C., Eichhorn, S.W., Thiru, P., Ghazvinian, R., George, T.I., Gotlib, J.R., Beggs, A.H., Sieff, C.A., et al. (2014). Altered translation of GATA1 in Diamond-Blackfan anemia. Nat. Med. *20*, 748–753.

Ludwig, L.S., Lareau, C.A., Bao, E.L., Nandakumar, S.K., Muus, C., Ulirsch, J.C., Chowdhary, K., Buenrostro, J.D., Mohandas, N., An, X., et al. (2019). Transcriptional States and Chromatin Accessibility Underlying Human Erythropoiesis. Cell Rep. *27*, 3228-3240.e7.

Lukassen, S., Chua, R.L., Trefzer, T., Kahn, N.C., Schneider, M.A., Muley, T., Winter, H., Meister, M., Veith, C., Boots, A.W., et al. (2020). SARS □CoV□2 receptor ACE 2 and TMPRSS 2 are primarily expressed in bronchial transient secretory cells . EMBO J. *39*, 1–15.

Mello, F. V., Land, M.G.P., Costa, E.S., Teodósio, C., Sanchez, M.L., Bárcena, P., Peres, R.T., Pedreira, C.E., Alves, L.R., and Orfao, A. (2019). Maturation-associated gene expression profiles during normal human bone marrow erythropoiesis. Cell Death Discov. *5*:69.

Pellegrini, L., Albecka, A., Mallery, D.L., Kellner, M.J., Paul, D., Carter, A.P., James, L.C., and Lancaster, M.A. (2020). SARS-CoV-2 infects the brain choroid plexus and disrupts the blood-CSF-barrier in human brain organoids. Cell Stem Cell 27(6):951-961.

Ropa, J., Cooper, S., Capitano, M.L., Van't Hof, W., and Broxmeyer, H.E. (2020). Human

Hematopoietic Stem, Progenitor, and Immune Cells Respond Ex Vivo to SARS-CoV-2 Spike Protein. Stem Cell Rev. Reports. Oct 21, 1-13.
Shahbaz, S., Xu, L., Osman, M., Sligl, W., Shields, J., Joyce, M., Tyrrell, L., Oyegbami, O., and Elahi, S. (2020). Erythroid precursors and progenitors suppress adaptive immunity and get invaded by SARS-CoV-2. BioRxiv 2020.08.18.255927.
Sungnak, W., Huang, N., Bécavin, C., Berg, M., Queen, R., Litvinukova, M., Talavera-López, C., Maatz, H., Reichart, D., Sampaziotis, F., et al. (2020). SARS-CoV-2 entry factors are highly expressed in nasal epithelial cells together with innate immune genes. Nat. Med. *26*, 681–687.
Vabret, N., Britton, G.J., Gruber, C., Hegde, S., Kim, J., Kuksin, M., Levantovsky, R., Malle, L., Moreira, A., Park, M.D., et al. (2020). Immunology of COVID-19: Current State of the Science. Immunity *52*, 910–941.
Varatharaj, A., Thomas, N., Ellul, M.A., Davies, N.W.S., Pollak, T.A., Tenorio, E.L., Sultan, M., Easton, A., Breen, G., Zandi, M., et al. (2020). Neurological and neuropsychiatric complications of COVID-19 in 153 patients: a UK-wide surveillance study. The Lancet Psychiatry *7*, 875–882.
Walls, A.C., Park, Y.J., Tortorici, M.A., Wall, A., McGuire, A.T., and Veesler, D. (2020). Structure, Function, and Antigenicity of the SARS-CoV-2 Spike Glycoprotein. Cell *181*, 281-292.e6.
Wang, Y., Liu, S., Liu, H., Li, W., Lin, F., Jiang, L., Li, X., Xu, P., Zhang, L., Zhao, L., et al. (2020). SARS-CoV-2 infection of the liver directly contributes to hepatic impairment in patients with COVID-19. J. Hepatol. *73*, 807–816.
Westers, T.M., Cremers, E.M.P., Oelschlaegel, U., Johansson, U., Bettelheim, P., Matarraz, S., Orfao, A., Moshaver, B., Brodersen, L.E., Loken, M.R., et al. (2017). Immunophenotypic analysis of erythroid dysplasia in myelodysplastic syndromes. A report from the IMDSFlow working group. Haematologica *102*, 308–319.
Wu, J., Song, S., Cao, H.C., and Li, L.J. (2020). Liver diseases in COVID-19: Etiology, treatment and prognosis. World J. Gastroenterol. *26*, 2286–2293.
Yang, L., and Tu, L. (2020). Implications of gastrointestinal manifestations of COVID-19. Lancet Gastroenterol. Hepatol. *5*, 629–630.
Zhang, B.Z., Chu, H., Han, S., Shuai, H., Deng, J., Hu, Y. fan, Gong, H. rui, Lee, A.C.Y., Zou, Z., Yau, T., et al. (2020). SARS-CoV-2 infects human neural progenitor cells and brain organoids. Cell Res. *30*, 928–931.

FIGURE LEGENDS

Figure 1. COVID19 patients show symptoms of disruptive erythropoiesis and ACE2 is highly expressed in erythroid progenitors

(A and B) Monitoring of the hemoglobin levels (A) and nucleated red blood cells (B) during the first 28 days post hospitalization at King's College Hospital. Data represents the mean value of the 30 patients for each day.

(C) ACE2 expression during *in vitro* erythropoiesis (from GSE118537). Each bar represents the normalized counts for ACE2 of each individual sample during the time course.

(D) Principal component analysis of GSE118537 dataset with the 3 subpopulations analyzed. Time points of Stage 1 are represented in pink, time points of Stage 2 in red and time points of Stage 3 in garnet.

(E) Expression level of ACE2 and classical markers to define HSPCs and erythroid progenitors in S1, S2 and S3. Each dot represents one sample of the time course.

(F) Representative gating strategy from bone marrow to define ERP-S1, ERP-S2 and ERP-S3. Lineage cocktail includes CD14, CD16 and CD19.
(G) Percentage of each erythroid progenitor in the mononuclear cell fraction of each tissue analyzed (CB: cord blood, BM: bone marrow, PB: peripheral blood). Each dot represents one independent human donor. Two-way ANOVA test was used for the comparison among the three tissues; **$p < 0.01$; ***$p < 0.005$.

Figure 2. Isolation and analysis of erythroid progenitors co-expressing ACE2 and TMPRSS2.
(A) Schematic of sample processing: human bone marrow or peripheral blood were processed to isolate by cell sorting ERP populations. ACE2 and TMPRSS2 at the cell membrane was analyzed by confocal microscopy. SARS-CoV-2 infectivity was quantified by the detection of three viral genes (N: Nucleocapsid, E: Envelope and RdRP: RNA-dependent Polymerase) by RT-qPCR. Created with BioRender.
(B) Immunostaining and fluorescence intensity quantification of ACE2 and TMPRSS2 in HSPCs and erythroid progenitors (ERPs) (scale-bar 10 µm). Each dot represents one cell; HSPCs (351 cells), ERP-S1 (50 cells), ERP-S2 (48 cells), ERP-S3 (106 cells). This is representative of one of the two independent immunostainings performed. Two-way ANOVA test was used for the comparison among the different cell populations; ****$p < 0.001$.

Figure 3. SARS-CoV-2 infects erythroid progenitors and can be detected in erythroid colonies 14 days later.
(A) SARS-CoV-2 infection at MOI 5 in ERPs from bone marrow. Quantification by RT-qPCR of the Nucleocapsid (N), Envelope (E) and RNA-dependent RNA Polymerase (RdRP) SARS-CoV-2 genes at 24 hours post-infection. Each dot represents an independent biological donor (n=3). Values represent ΔΔCt normalized to GAPDH. Error bars show the mean ± SD. Two-way ANOVA test was used for the comparison among the different cell populations; *$p < 0.05$; **$p < 0.01$; ***$p < 0.005$; ****$p < 0.001$; ns: no significance.
(B) Replication of SARS-CoV-2 genes between 30 minutes and 24 hours post infection. Each dot represents an independent biological donor (n=3). Values represent the differences in ΔΔCt normalized to GAPDH between the quantification of viral genes at 24h and quantification after 30 minutes of viral infection. Error bars show the mean ± SD. Two-way ANOVA test was used for the comparison among the different cell populations; *$p < 0.05$; **$p < 0.01$; ***$p < 0.005$; ****$p < 0.001$.
(C) Colony-forming unit (CFU) assay of ERPs after 24 hours in culture with the virus. Data represents total number of colonies per 1000 ERP-S1 cells (left panel) or ERP-S2 cells (right panel). 4000 cells of each population were seeded in triplicates in methylcellulose plates and colonies were counted 14 days later. Each dot represents an independent biological donor (n=3). Error bars show the mean ± SD. T-test was used for the comparison between the different conditions of each sample; *$p < 0.05$.
(D) SARS-CoV-2 detection (N gene) in 10 independent colonies from ERP-S1 or ERP-S2 plates. After 14 days we pick colonies, extract RNA and analyze by RT-qPCR the presence of the virus. Data represents the mean ± SD of the RT-qPCR triplicates for each independent colony of one experiment.

Figure 1

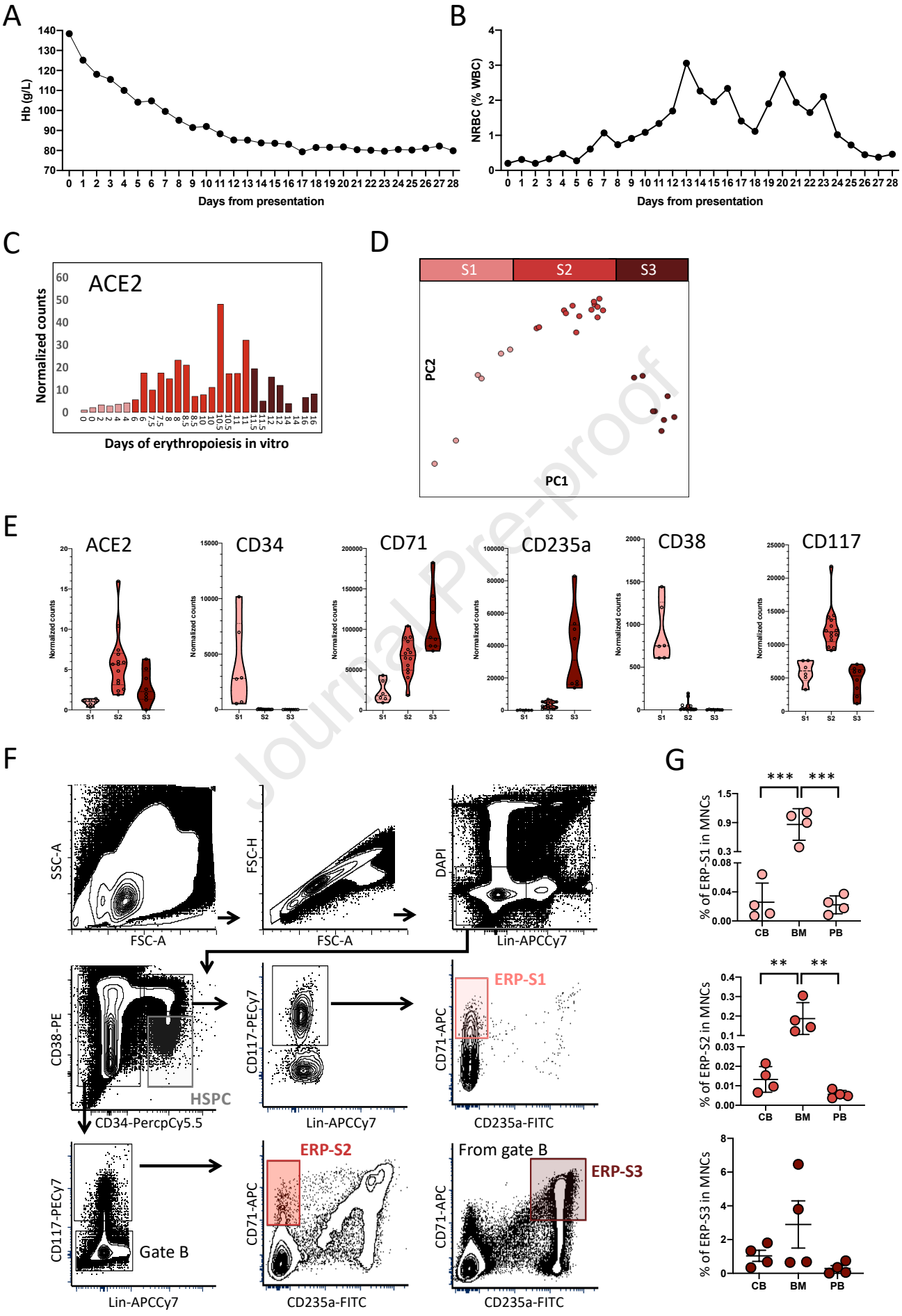

Figure 2

A

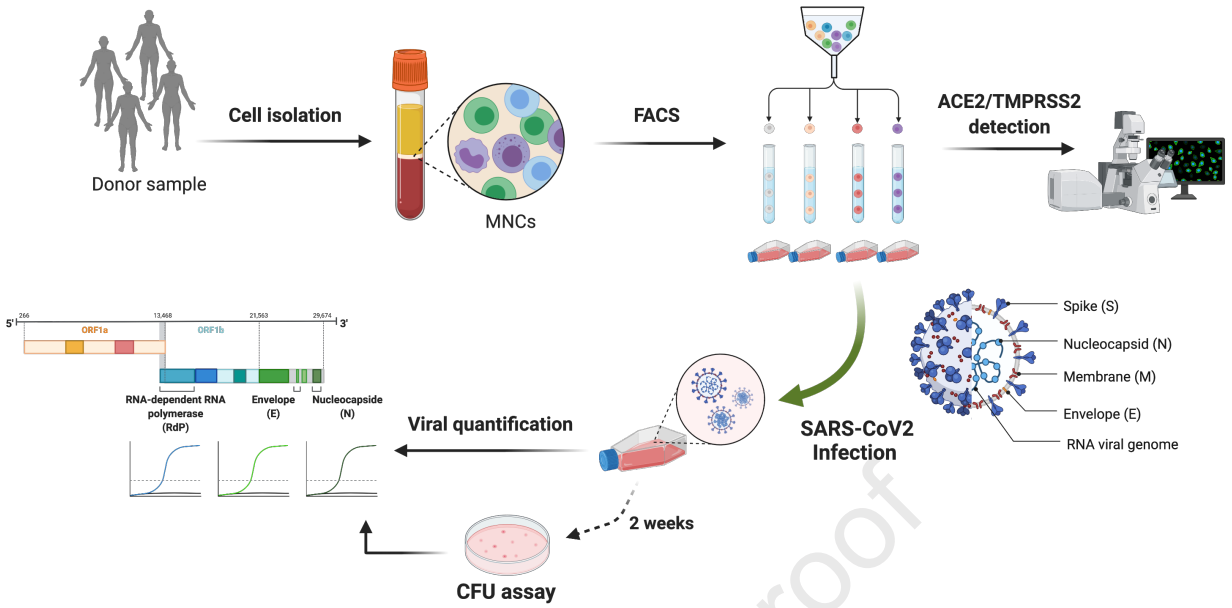

B

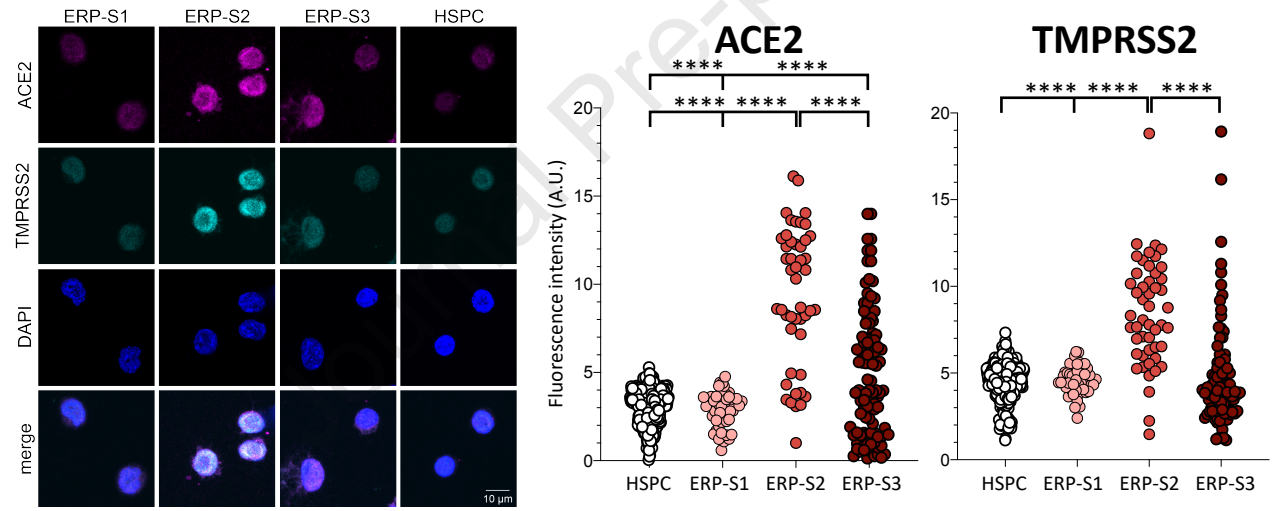

Figure 3

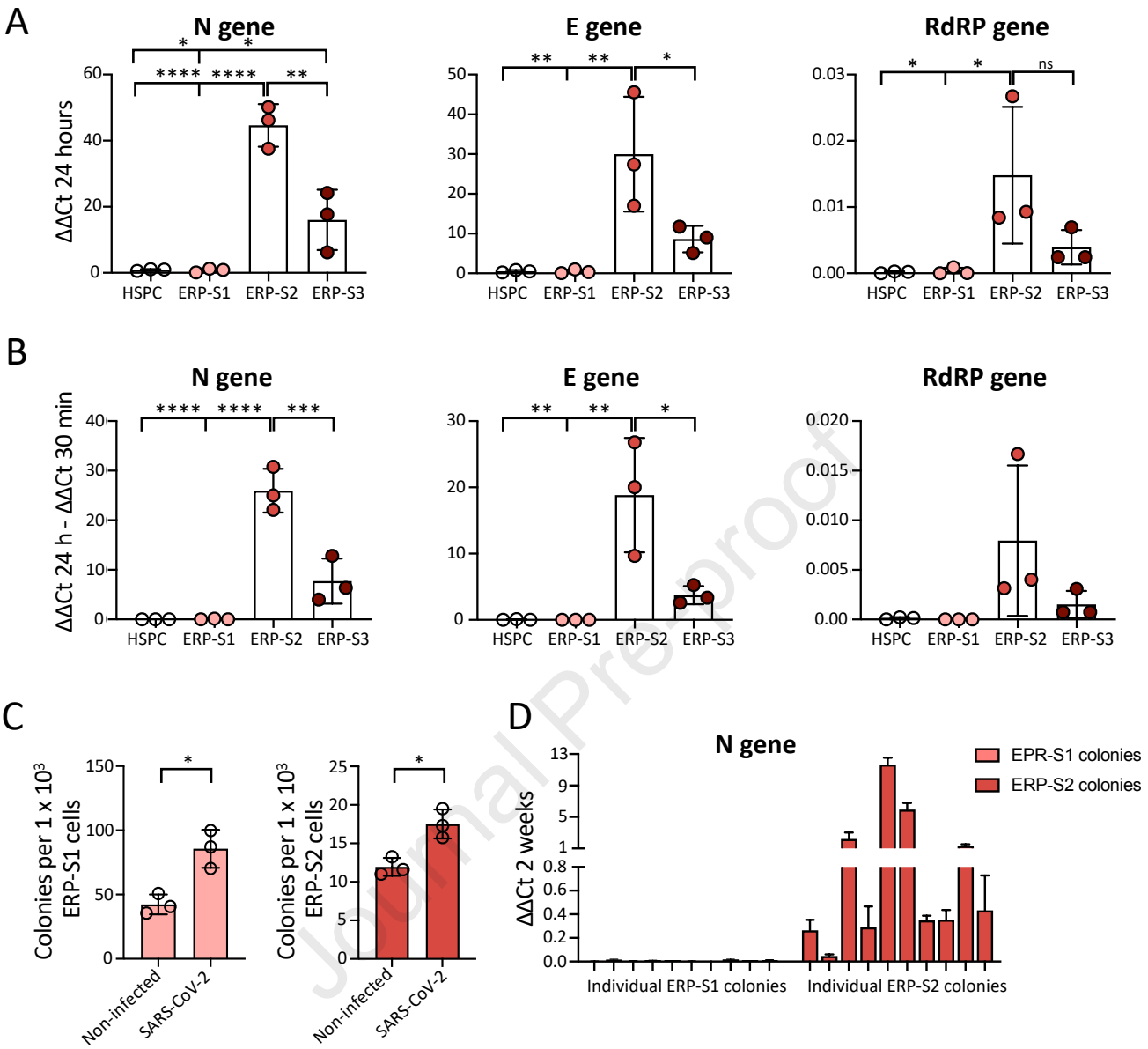

Highlights:

- Patients with severe COVID19 symptoms show severe anemia and increase in nucleated red blood cells.
- Erythroid progenitors co-express ACE2 and TMPRSS2.
- Early, and to a lesser extend mid-late, erythroid progenitors could be infected by SARS-CoV-2.
- SARS-CoV-2 can be detected in erythroid colonies 14 days after the initial infection.

TOC blurb

H.H. Encabo and colleagues demonstrate that SARS-CoV-2 can infect erythroid progenitors without impairing their functionality, rather causing an expansion of colonies where the virus can be detected. These findings shed light into the severe COVID-19 patients who suffer from an aberrant increase of nucleated red blood cells concomitant with reduced levels of hemoglobin.